Bowhead whale localization using time-difference-of-arrival data from asynchronous recorders

Graham A. Warner[a] and Stan E. Dosso
School of Earth and Ocean Sciences, University of Victoria, 3800 Finnerty Road, Suite 405A, Victoria, British Columbia V8P 5C2, Canada

David E. Hannay
JASCO Applied Sciences, 2305-4464 Markham Street, Victoria, British Columbia V8Z 7X8, Canada

(Received 2 August 2016; revised 6 February 2017; accepted 27 February 2017; published online 20 March 2017)

This paper estimates bowhead whale locations and uncertainties using nonlinear Bayesian inversion of the time-difference-of-arrival (TDOA) of low-frequency whale calls recorded on onmidirectional asynchronous recorders in the shallow waters of the northeastern Chukchi Sea, Alaska. A Y-shaped cluster of seven autonomous ocean-bottom hydrophones, separated by 0.5–9.2 km, was deployed for several months over which time their clocks drifted out of synchronization. Hundreds of recorded whale calls are manually associated between recorders. The TDOA between hydrophone pairs are calculated from filtered waveform cross correlations and depend on the whale locations, hydrophone locations, relative recorder clock offsets, and effective waveguide sound speed. A nonlinear Bayesian inversion estimates all of these parameters and their uncertainties as well as data error statistics. The problem is highly nonlinear and a linearized inversion did not produce physically realistic results. Whale location uncertainties from nonlinear inversion can be low enough to allow accurate tracking of migrating whales that vocalize repeatedly over several minutes. Estimates of clock drift rates are obtained from inversions of TDOA data over two weeks and agree with corresponding estimates obtained from long-time averaged ambient noise cross correlations. The inversion is suitable for application to large data sets of manually or automatically detected whale calls. © *2017 Acoustical Society of America*. [http://dx.doi.org/10.1121/1.4978438]

[AMT] Pages: 1921–1935

I. INTRODUCTION

Localizing marine mammals is important for estimating their distributions and movement. Passive acoustic monitoring can be used to infer the presence and location of vocalizing marine mammals over long time periods using autonomous underwater recorders to record calls from animals over large areas. Many localization techniques rely on recorder synchronization, but the clocks in low-power underwater recorders are susceptible to temperature changes and tend to drift out of synchronization with respect to each other over long-duration deployments. Widely distributed asynchronous directional sensors can be used to localize marine mammals,[1–3] but the equipment is typically more expensive and difficult to deploy and calibrate than onmidirectional hydrophones, and is therefore often not used. Even when complex equipment such as synchronized vertical or horizontal arrays are available,[3–5] the computational cost of numerical wave-equation based acoustic propagation models can be high. This paper presents a nonlinear Bayesian inversion for localizing bowhead whales in the Chukchi Sea using call time-difference-of-arrival (TDOA) data derived from low-frequency calls recorded on omnidirectional asynchronous seabed recording systems.

TDOA localization methods have been developed and used extensively over the last ∼50 yr for localizing marine mammals with synchronized recorders at known locations.[6–17] For example, TDOA between multi-path arrivals of sperm-whale clicks (high-frequency, impulsive sources) have been used to localize whales in three dimensions.[15] However, much less attention has been given to localizing animals based on low-frequency, non-impulsive calls in shallow-water environments where propagation is modal, which is the goal of the present work.

The localization problem is more difficult with unsynchronized recorders and difficulties are further compounded if the recorder locations and/or water sound speed are uncertain.[18] Recorder synchronization is often performed by assuming a linear clock drift between deployment and recovery,[19] but this may not accurately reflect the true clock drift especially during periods of rapid temperature change (e.g., upon deployment and recovery). Sabra *et al.*[20] showed that ambient noise can be used to synchronize and locate array elements using cross correlations if the local sound speed is known and the noise sources are distributed uniformly in azimuth. This technique has been successfully applied to small-aperture arrays;[21] however, the large averaging times required for wide-aperture arrays can preclude synchronization if the clocks drift significantly over the duration required to build the time-domain Green's function (derivative of the cross correlation between receivers). Equipping recorders with global positioning system (GPS) devices can provide accurate timing and position information[22–25] but require a GPS receiver at the sea surface, which may not be practical/possible in all environments (e.g., ice-covered waters).

[a]Electronic mail: gwarner@uvic.ca

Recorders with chip-scale atomic clocks can stay adequately synchronized over long time periods but have been much more expensive than recorders without atomic clocks.

A previous study involving an unsynchronized wide-aperture array estimated bowhead whale locations and recorder clock drifts using Bayesian inversion of modal dispersion data.[26] That approach was based on extracting dispersion data (arrival times as a function of frequency) for multiple water-borne acoustic modes using a warping time-frequency analysis,[27] and inverting the data for whale locations, clock offsets, the instantaneous frequency function of each whale call, and environmental models (sound-speed profile of the water column and sound-speed and density profiles of the seabed). Sound propagation was modeled using a normal-mode code and the inversion used trans-dimensional Markov-chain Monte Carlo sampling[28] to account for the unknown number of layers in the sound-speed profile and seabed. Although that method was quite accurate, the computational expense of the propagation model and environmental inversion (as well as the manual effort in data processing) makes it challenging to apply the method to large numbers of whale calls. Similar modal-dispersion approaches for simpler one-dimensional range-estimation still require nontrivial manual data processing and a relatively complex and time-consuming propagation model.[27,29]

In this paper, we use a much simpler and faster (but generally less accurate) propagation/environmental model and a nonlinear Bayesian inversion to estimate bowhead whale locations using whale-call TDOA data (the inversions were 2–4 orders of magnitude faster per whale localization than the modal-dispersion inversion[26]). Acoustic propagation is modeled as time-of-flight along straight acoustic paths in the horizontal plane with an unknown effective sound speed. This propagation model has been applied previously for localizing bowhead and right whales using low-frequency calls recorded in shallow water with an assigned (estimated) effective sound speed held fixed in the localization.[13,30] Recently, Abadi *et al.*[31] applied this propagation model with unknown effective sound speed for localizing humpback whales. In that work, the unknown effective sound speed was accounted for by reducing the measured mean water-column sound speed by the mode-averaged incident angle, which was estimated using data from a synchronized wide-aperture horizontal array. In this paper we consider data from asynchronous recorders and formulate the problem to estimate the effective waveguide sound speed directly. In particular, the nonlinear inversion developed here considers the whale locations, relative recorder clock offsets, effective sound speed, and recorder locations as unknown parameters (with varying levels of prior information) that are all estimated simultaneously. The inversion also rigorously estimates residual error statistics and quantitative uncertainties for all parameters. We note that a corresponding linearized Bayesian inversion we developed was even faster but often did not produce physically realistic results, indicating that the inverse problem is strongly nonlinear.

The nonlinear inversion is applied here to batches of bowhead whale-call TDOA data (both simulated and measured) occurring over time periods which are short enough that the clocks do not drift significantly relative to each other ($\sim$30 min) compared to the magnitude of the TDOA data. A simulation study investigates how whale localization uncertainties, characterized by probability density functions (PDFs), are affected by the assumption that multiple calls propagate with the same effective sound speed, given that calls have potentially different frequency content and are emitted at different depths (hence, exciting modes differently), and environmental properties could vary spatially over the study region. The simulation study also investigates how localization uncertainties change with the number of recorders that detected each call and with the source-receiver geometry, as well as the degree to which the other parameters are constrained. The inversion is also applied to measured bowhead whale-call TODA data obtained from recordings of an underwater sound measurement program in the Chukchi Sea, Alaska.[32] Although the recorded bowhead whale calls clearly indicate modal dispersion, the dispersive (call spreading) effects are generally of much less significance than the differences in propagation times along different source/receiver paths. Hundreds of bowhead whale calls were manually annotated and associated from recordings of seven seabed-mounted recorders. The inversion results showed the recorder geometry was suitable for bowhead whale localization and estimating relative recorder clock offsets including long-term drift rates. Whale location uncertainties are often small enough to associate calls with distinct whales and track repetitively calling whales (or whale groups) with reasonable swim speed.

II. BOWHEAD WHALE-CALL DATA

Long-term underwater acoustic recordings were collected by JASCO Applied Sciences (Halifax, Nova Scotia, Canada) from August to October 2013, as part of an acoustic measurement program designed, in part, to record marine-mammal calls over a large area of the Chukchi Sea.[32] The recordings were made using 28 of JASCO's Autonomous Multichannel Acoustic Recorders (AMARs), which drifted out of synchronization with each other over the deployment period. Each recorder was equipped with a single Geospectrum M8E hydrophone (nominal sensitivity –164 dB re 1 V/μPa, Dartmouth, Nova Scotia, Canada) and recorded 24-bit samples at a 64 kHz sampling rate. Most recorders were spaced tens of kilometers apart; however, a cluster of closely spaced recorders was centered around Shell's (Anchorage, AK) 2012 drilling location to quantify sound levels from oil and gas exploration activities. Seven recorders (denoted by JASCO as BGA–BGE, BGH, and BGJ, but herein renamed as A–G, respectively) were deployed within 8 km of the drill site (71°18.5′N, 163°12.7′W) at nominal distances of 0.5, 1, 2, 4, and 8 km (three AMARs were deployed at 2-km range at different azimuths). Approximate AMAR locations were recorded upon deployment using GPS. The water depths at the seven AMAR deployment locations varied between 46.0 and 48.7 m.

Bowhead whales passed the AMAR cluster during their annual fall migration from the Beaufort and Chukchi Seas to the Bering Sea. The AMARs recorded thousands of bowhead calls (mostly at frequencies below 400 Hz) and many of the calls were detected on multiple AMARs in the cluster. The bowhead whale calls and other acoustic events (e.g., marine

seismic airgun pulses) were used to approximately synchronize the recorders by listening to the recordings and observing time-frequency characteristics of the events. Bowhead whale calls were detected manually on waveform and spectrogram displays and assigned start and end times relative to the corresponding recorder's clock, as well as lower and upper frequencies. For this study, we manually made 1926 annotations of 347 unique bowhead whale calls recorded on AMARs A–G during six half-hour time windows between 27 September and 11 October. The same call was identified on multiple AMAR recordings by listening to the recordings and observing corresponding spectrograms of the call; however, most calls were not identified on all AMARs. For each call, corresponding detections on the recorders were associated by assigning the same unique call name to each annotation. Figure 1 shows an example of spectrograms from each AMAR during a 90-s period on 3 October.

III. THEORY

A. Data processing

Call waveforms were bandpass filtered within their assigned lower and upper frequencies using Butterworth filters. Filtered waveforms were then cross-correlated with detections of the same call from other recorders. In this paper, we consider whale calls recorded at up to seven recorders, which yields up to 21 cross-correlation functions per call. The envelopes of the normalized cross-correlation functions were computed and the TDOAs were determined by the time delay of the envelope's maximum.[16] The TDOAs were sorted in descending order by the maximum values of the envelopes and the first two and up to six linearly independent TDOAs were saved for the inversion (linearly dependent TDOAs were discarded). This was done because using linearly dependent TDOA is inconsistent with the assumptions of independent data errors (described in Sec. III C) and could result in underestimating uncertainties in the whale locations. It also reduced the influence of call dispersion on TDOA data (not accounted for in the propagation model), as higher cross-correlation maxima favored similarly-dispersed calls which yielded more-accurate TDOA data.

B. Bayesian inversion

The call arrival times depend on the whale and receiver locations, time of the call, and relative recorder clock offsets. Using a simple straight-path, time-of-flight propagation model,[13,30,31] the arrival time for call w at recorder i is

$$t_{wi} = \tau_w + \frac{\sqrt{(x_w - X_i)^2 + (y_w - Y_i)^2}}{c} + \Delta_i, \tag{1}$$

where τ_w is the time of the whale call, x_w and y_w are the easting and northing coordinates of the whale, X_i and Y_i are the coordinates of the recorder, c is the effective waveguide sound speed (discussed below), and Δ_i is the (static) recorder

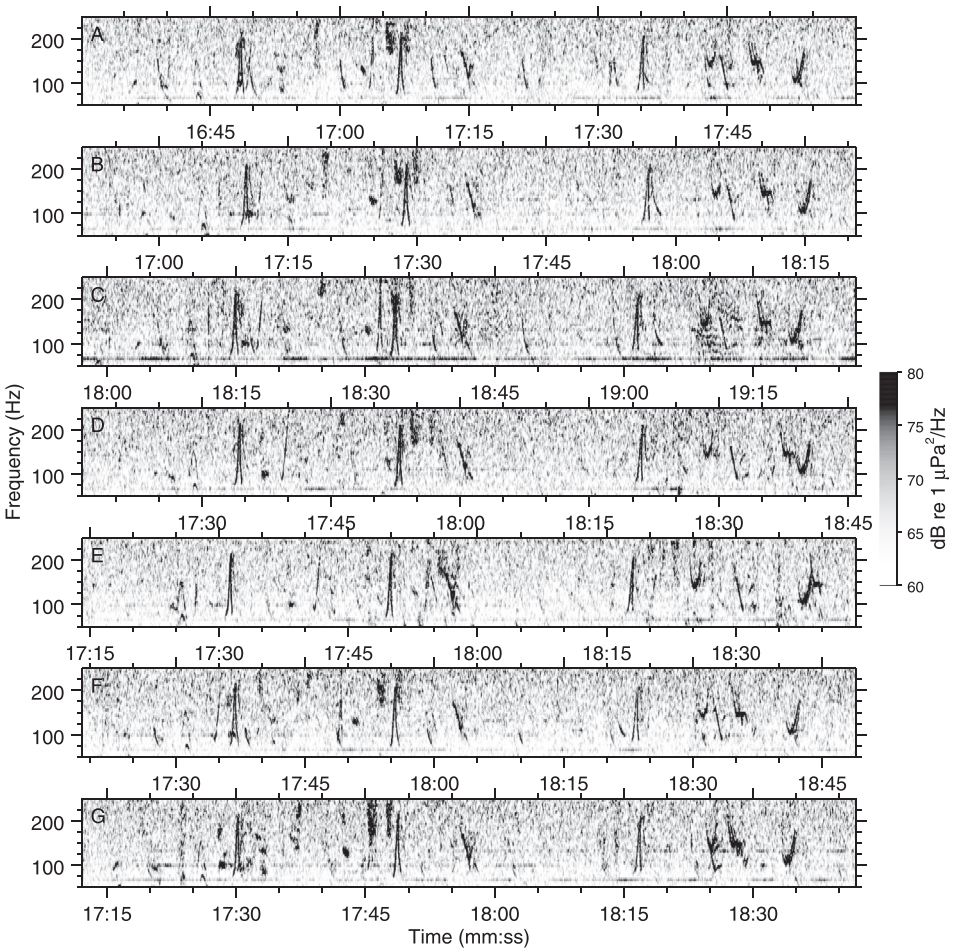

FIG. 1. Spectrograms of bowhead whale calls recorded on AMARs A–G on 3 Oct. Times are given in minutes and seconds after midnight for each AMAR clock. Note that the relative recorder clock offsets are much larger than any physically realistic propagation effect but it is still possible to (approximately) time-align the recordings.

clock offset relative to a reference recorder. The bowhead whale calls analyzed for this paper propagate as normal modes in the shallow-water environment. The sound speed c is therefore an effective average modal group speed (less than the water sound speed) weighted by the frequency and modal content of the calls (the latter is also dependent on source depth). Section IV carries out a simulation study to investigate the effects of assuming a single call-independent effective sound speed in the inversion, given realistic variations in the sound speed in producing the data. The conclusion is that a call-independent sound speed is sufficient, as assumed in the theory developed in this section. Considering TDOAs for a whale call recorded at receivers i and j removes the dependence on whale call time, as given by

$$t_{wi} - t_{wj} = \frac{\sqrt{(x_w - X_i)^2 + (y_w - Y_i)^2}}{c} - \frac{\sqrt{(x_w - X_j)^2 + (y_w - Y_j)^2}}{c} + \Delta_i - \Delta_j. \quad (2)$$

The Bayesian inversion estimates the unknown model parameters $\mathbf{m} = [x_1, \ldots, x_W, y_1, \ldots, y_W, X_1, \ldots, X_R, Y_1, \ldots, Y_R, \Delta_2, \ldots, \Delta_R, c]^T$, where W is the number of whale calls, R is the number of recorders (with recorder 1 as the reference recorder so $\Delta_1 = 0$). In addition, the error standard deviation is also considered unknown and treated as described in Sec. III C. The inversion is carried out by sampling the posterior probability density (PPD) of the model parameters, given the measured data and prior information, with Metropolis-Hastings sampling,[33,34] a Markov-chain Monte Carlo (MCMC) algorithm. Parallel tempering[35–38] and parameter rotation[39] are used to efficiently sample complicated potentially multi-modal PPD structure, which involve highly correlated parameters. Parameter rotation is implemented for all model parameters using eigenvalue decomposition of the posterior model covariance matrix (estimated using previous MCMC samples) and perturbing the current model along randomly selected eigenvectors using symmetric Cauchy proposal densities scaled by the corresponding eigenvalues. The model transition acceptance probability is applied after perturbing the current model and depends on the prior, proposal, and likelihood ratios.[33,34,40,41] Uniform (bounded) prior probability densities are used for all model parameters and symmetric probability densities are used for the proposals, reducing the model transition acceptance probability to the likelihood ratio (Sec. III C).

The upper (prior) bound for sound speed was set to be the maximum expected water sound speed in the area during September and October.[42–44] The minimum sound speed was approximately the lowest group speed of mode 3 as estimated using environmental properties from a previous inversion of bowhead whale modal-dispersion data recorded on the same hydrophones.[26] Mode 3 was the highest-order mode observed in the annotated calls. Recorder locations (easting and northing) were allowed to vary in the inversion by up to 50 m from their GPS-based deployment locations to account for recorder-location uncertainty. The intent here is not so much to localize the recorders as to quantitatively account for receiver-location uncertainties in the whale localization uncertainties. Relative recorder clock offsets were allowed to vary by up to 5 s from the median of all TDOAs for each recorder.

C. Likelihood

The likelihood function is defined by the residual error PDF. Measurement, data-processing, and theory errors comprise residual errors and their PDFs are often unknown. Residual errors for model $\mathbf{m}$ are given by $\mathbf{d} - \mathbf{d}(\mathbf{m})$, where $\mathbf{d}$ and $\mathbf{d}(\mathbf{m})$ are the measured and predicted (TDOA) data, respectively. We assume residual errors are independent and Gaussian-distributed in this paper, the validity of which is checked *a posteriori*. For N data, the corresponding likelihood function is

$$L(\mathbf{m}) = \frac{1}{(2\pi)^{N/2}\sigma^N} \exp\left[-\frac{|\mathbf{d} - \mathbf{d}(\mathbf{m})|^2}{2\sigma^2}\right], \quad (3)$$

where σ is the error standard deviation. Setting $\partial L/\partial\sigma = 0$ leads to a maximum-likelihood estimate for the error standard deviation σ,

$$\hat{\sigma}(\mathbf{m}) = \left[|\mathbf{d} - \mathbf{d}(\mathbf{m})|^2/N\right]^{1/2}. \quad (4)$$

Equation (4) expresses σ in terms of the data and other unknown model parameters, allowing implicit sampling of $\hat{\sigma}$ by sampling explicitly over the parameters in $\mathbf{m}$.[45]

IV. SIMULATION STUDY

This section illustrates the capabilities and limitations of the TDOA localization in simulations based on bowhead-whale recordings in the Chukchi Sea (described in Sec. II). First, to investigate the effect of source depth on the effective waveguide sound speed, we simulated the propagation of bowhead whale calls originating at different depths. We used the normal mode code ORCA[46] and Fourier synthesis to create synthetic time series representing bowhead calls for source depths near the surface (2-m depth), mid water column (20 m), and near the seafloor (42 m) to receivers 1 m above the seafloor and at ranges of 1, 2, 4, and 8 km. The source waveform was taken from a close-range recording of a downswept (85–45 Hz) bowhead whale call [see Fig. 7(d) in Warner *et al.*[26]] and the environmental model was taken from Warner *et al.*[26] where the water depth was 46 m. Simulated waveforms were processed as described in Sec. III A for all pairs of the four simulated received signals. The recorder separation distance was divided by the TDOA to calculate the effective waveguide sound speed (for this simulation we assume the recorders and source are in-line and their locations are exactly known). The mean effective waveguide sound speeds for sources at 2, 20, and 42 m depth were 1362, 1381, and 1386 m/s with standard deviation of 41, 47, and 41 m/s, respectively. The near-surface source generally results in the lowest sound speed as it excites higher-order modes; however, the speeds are essentially indistinguishable given the variability. Furthermore, the

TABLE I. True model parameters and corresponding prior bounds for simulations 1–3. The (single) sound speed for all calls in simulation 3 was 1400 m/s. Priors given with "±" indicate bounds relative to the true parameters.

Parameter	True value(s)	Prior bounds
c (m/s)	[1338,1410,1377,1448,1362,1362,1398,1346,1407,1394,1403,1318]	[1300,1465]
Δ_{B-G} (s)	[−51, −53, −5, 31, 11, −59]	±5
x_w (km)	[1.7, 8.1, 23.5, 0.1, −3.7, −2.9, −1.1, −11.9, −2.6, 5.7, −7.5, 4.7]	[−30, 30]
y_w (km)	[2.4, 5.2, 16.7, 4.5, 8.2, 16.2, −0.6, 1.2, −7.7, −1.8, −15.5, 2.7]	[−30, 30]
X_{A-G} (m)	[0, 419, 1297, 3011, 6507, −424, −2154]	±50
Y_{A-G} (m)	[0, 246, 773, 1790, 3767, −2232, 754]	±50

variability in effective waveguide sound speed for different receiver pairs and a fixed source depth is relatively large, indicating that the cross-correlation data processing method for obtaining TDOAs is sensitive to changes in the modal content of calls with distance (e.g., from modal attenuation). This variability suggests it would be difficult to resolve call-dependent speeds in the present work.

To investigate the effects of call-dependent effective waveguide sound speeds on localization performance, we conducted three inversions of TDOA data. Simulation 1 considered TDOA data generated with call-dependent sound speeds that were inverted assuming call-dependent sound speeds (i.e., an unknown sound speed for each call was included in the model for the inversion). Simulation 2 considered the same TDOA data as simulation 1 except the data were inverted assuming a single (call-independent) sound speed. Simulation 3 considered TDOA data generated with a call-independent sound speed that were inverted assuming a call-independent sound speed. The simulations considered 12 simulated calls detected on up to 7 asynchronous recorders (A–G). The recorder locations were set to the Universal Transverse Mercator coordinates of the deployed recorder cluster[32] (with

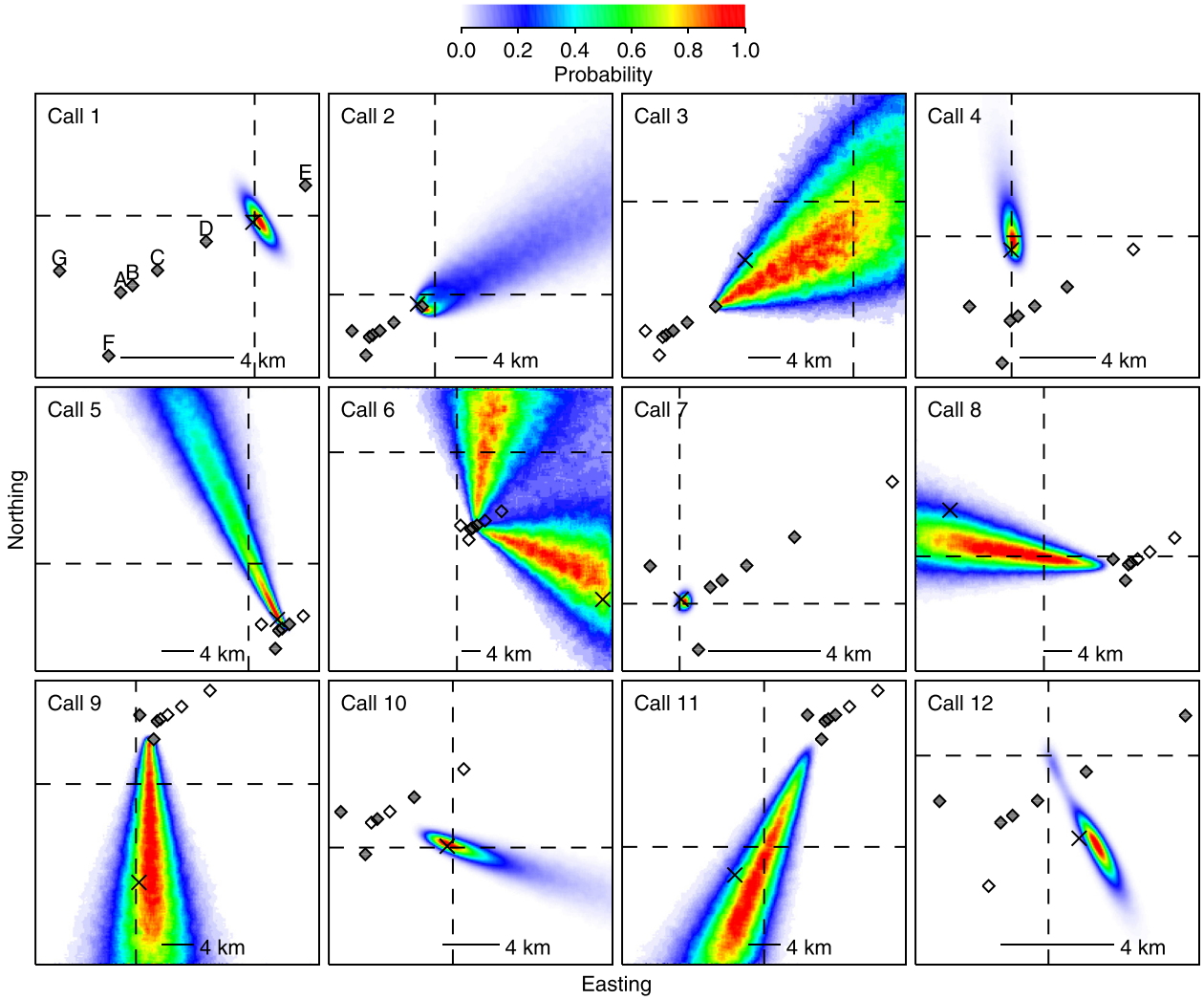

FIG. 2. (Color online) Amplitude-normalized marginal probability densities of simulated whale locations for calls 1–12 in simulation 1 (i.e., the inversion estimates call-dependent sound speeds for TDOA generated with call-dependent sound speeds). *A priori* recorder locations (simulated GPS deployment positions) are shown with diamond symbols; filled diamonds indicate recorders with TDOA data, open diamonds represent recorders without an associated call. MAP whale locations are shown with "×" symbols. The intersection of the dashed lines indicates true whale locations. Receivers A–G are identified for call 1.

the origin at recorder A) to investigate how the source-receiver geometry affects location uncertainty. TDOAs were simulated using Eq. (2) with true model parameters listed in Table I (simulation 3 used a single sound speed of 1400 m/s for all calls). Data were simulated for a minimum of three and up to all seven recorders, depending on the call (Fig. 2 shows the true simulated whale locations and the recorders that detected each call). Both TDOA datasets used the same recorders that detected each call. Linearly dependent data (combinations of receiver pairs) were removed on the basis of larger path length differences from source to receiver. This was done to simulate the expected effect of decreasing peak cross-correlation values between recorded calls in a dispersive waveguide, as discussed in Sec. III A. Gaussian-distributed independent zero-mean random errors with standard deviation 0.12 s were added to the true (simulated) data, which is consistent with standard deviations estimated for the measured whale-call data in Sec. V. For each scenario, the synthetic (noisy) data were inverted for the unknown parameters with prior bounds listed in Table I. Approximately 400 000 samples were drawn from the PPD via Metropolis-Hastings sampling, after a suitable burn-in period.

Figures 2 and 3 show the two-dimensional (2D) marginal probability densities for whale locations, the most-probable or maximum *a posteriori* (MAP) whale locations, and the true locations for all 12 simulated calls in simulations 1 and 2, respectively. The localization uncertainties depend strongly on the whale location relative to the receivers that recorded its call (indicated by filled diamonds), and the location uncertainty generally decreases as the number of recorders that detected the call increases. The probability densities are reasonably well constrained in two dimensions for calls 1, 4, 7, 10, and 12, whereas PDFs for calls 2, 3, 5, 8, 9, and 11 are constrained in bearing but poorly constrained in range from the recorders. The probability densities for calls 3 and 6 are the least constrained, being symmetric about the main recorder axis since the off-axis recorders F and G did not receive these calls. The PDF for call 12 is multi-modal with the southeastern mode having higher probability than the northwestern mode; however, the true call location is within the northwestern mode. This situation is more likely to occur when only one of the off-axis recorders (F or G) detects the call. Resolving this multi-

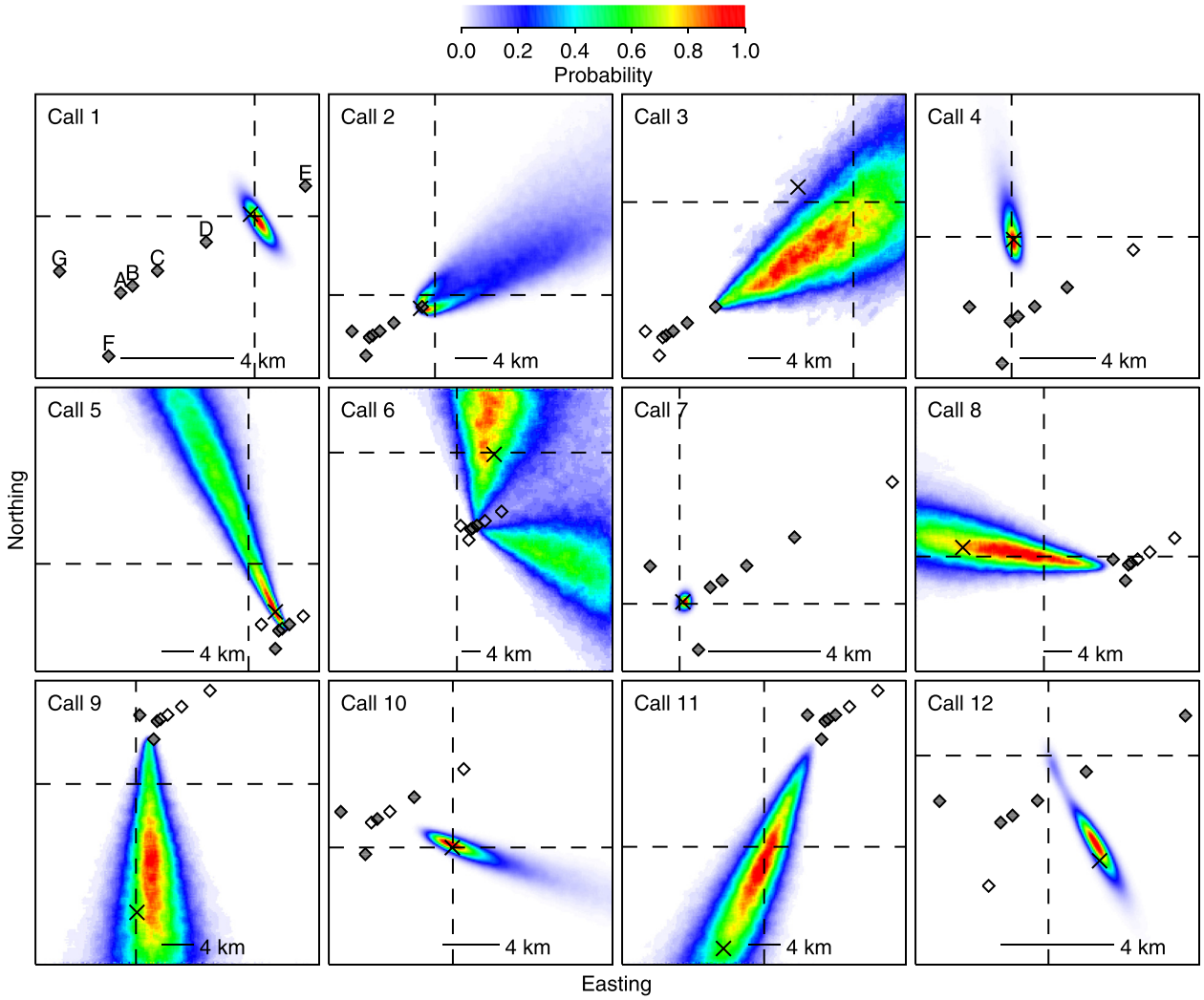

FIG. 3. (Color online) Amplitude-normalized marginal probability densities of simulated whale locations for calls 1–12 in simulation 2 (i.e., the inversion estimates a single call-independent sound speed for all calls even though the TDOA data were generated with call-dependent sound speeds). *A priori* recorder locations (simulated GPS deployment positions) are shown with diamond symbols; filled diamonds indicate recorders with TDOA data, open diamonds represent recorders without an associated call. MAP whale locations are shown with "×" symbols. The intersection of the dashed lines indicates true whale locations. Receivers A–G are identified for call 1.

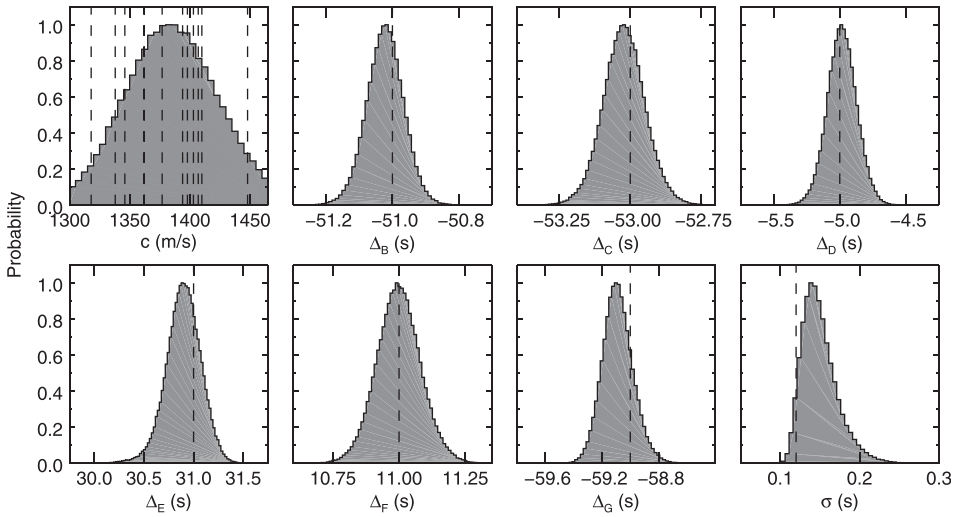

FIG. 4. Amplitude-normalized marginal probability densities for effective sound speed, relative recorder clock offsets, and residual error standard deviation for simulation 2. True values are indicated with dashed lines (all 12 call sound speeds are shown here with the single PDF for sound speed estimated in the inversion).

modal PPD structure illustrates the usefulness of the nonlinear Bayesian inversion approach since linearized inversion would produce a PPD with a single Gaussian mode about the MAP estimate and miss the true location in this example. Further, many of the marginal PPDs in Figs. 2 and 3 (and other localizations in this paper) are strongly non-Gaussian.

Importantly, the PDFs for simulations 1 and 2 in Figs. 2 and 3 are very similar, and the localization results for simulation 3 (not shown here for brevity) are very similar to these figures (about the same level of differences as those between Figs. 2 and 3). These results indicate that variations in the effective sound speed between different whale calls does not significantly affect the accuracy of whale localizations, and that the simplification of treating all calls as having the same effective sound speed is justified.

The influence of sound speed variations on TDOA data is generally of much less significance than relative recorder clock offset. For absolute travel-time measurements, variations in sound speed can cause large timing errors since they apply over the entire path length. For travel-time differences, however, sound speed variations only apply to the differences in path lengths to receivers, which are often much less than the path lengths themselves.

Figure 4 shows amplitude-normalized marginal probability densities for effective waveguide sound speed, relative recorder clock offsets, and residual-error standard deviation from simulation 2. The call-independent sound speed estimated by the inversion has a wide distribution with mean and standard deviation of 1384 and 35 m/s, respectively, and encompasses all 12 sound speeds used in generating the data. The marginal densities for all other values are peaked near the true values with the relative recorder clock offsets estimated with uncertainties of a few tenths of seconds. The corresponding figures for scenarios 1 and 3 are not shown for brevity, but are very similar to Fig. 4 except for sound speed. In scenario 1, the individual call-dependent sound speeds were poorly resolved; the PDFs were uninformative with mean standard deviation of 45 m/s. In scenario 3, the call-independent sound speed PDF is similar to the sound speed PDF in Fig. 4 with mean and standard deviation of 1395 and 34 m/s, respectively. Marginal probability densities for recorder locations are approximately flat (not shown), indicating that the data do not resolve recorder locations within the prior bounds; however, recorder-location uncertainties are accounted for in the whale-location uncertainties.

Figure 5 shows a sample of the fit to the data for the first four calls with the synthetic (noisy) TDOA data and the 5th and 95th percentiles for estimated TDOAs, calculated from a random sample of 5000 models from the PPD of simulation 2. The TDOA data index number on the x axis is the index of the simulated and predicted TDOA data vectors [$\mathbf{d}$ and $\mathbf{d}(\mathbf{m})$, respectively] and represents TDOA data from different recorder pairs (e.g., indices 0–5 represent the call 1 TDOAs between recorder pairs AB, AF, AG, BC, CD, and DE). The observed and estimated TDOAs were reduced by the difference of the clock offset estimates (taken from the MAP model sample) so the percentile differences are perceptible. The inversion sampled models that produced

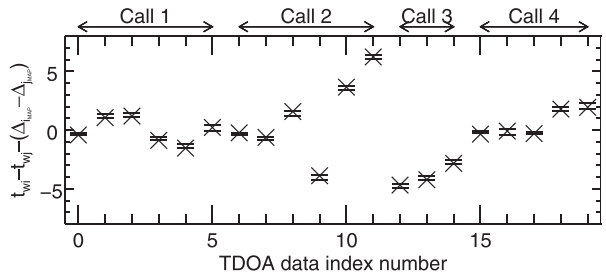

FIG. 5. Simulated (×) and predicted (–) TDOA data (s) for simulated whale calls 1–4 in simulation 2, reduced by the difference in relative recorder clock offsets from the MAP model. Predicted data are shown for the 5th and 95th percentiles of TDOA data from a random sample of the PPD.

TABLE II. Start dates and times for the six half-hour time windows analyzed for Chukchi Sea bowhead whale calls.

Scenario	Start date	Start time
S1	2013-09-27	00:30:00
S2	2013-09-27	01:00:00
S3	2013-09-27	01:30:00
S4	2013-10-03	00:00:00
S5	2013-10-06	00:00:00
S6	2013-10-11	03:39:00

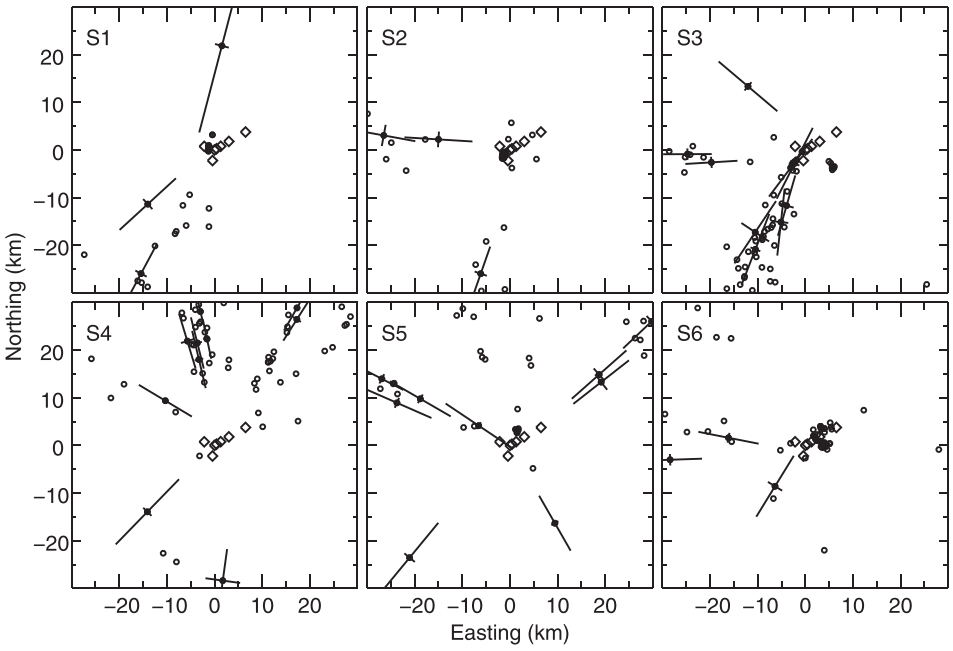

FIG. 6. Bowhead whale locations ("○" symbols) from the MAP models and 1SD uncertainty estimates (solid lines) along the principal-component axes of the location estimates for six randomly selected calls of each scenario. *A priori* AMAR locations (GPS deployment positions) are shown with diamond symbols.

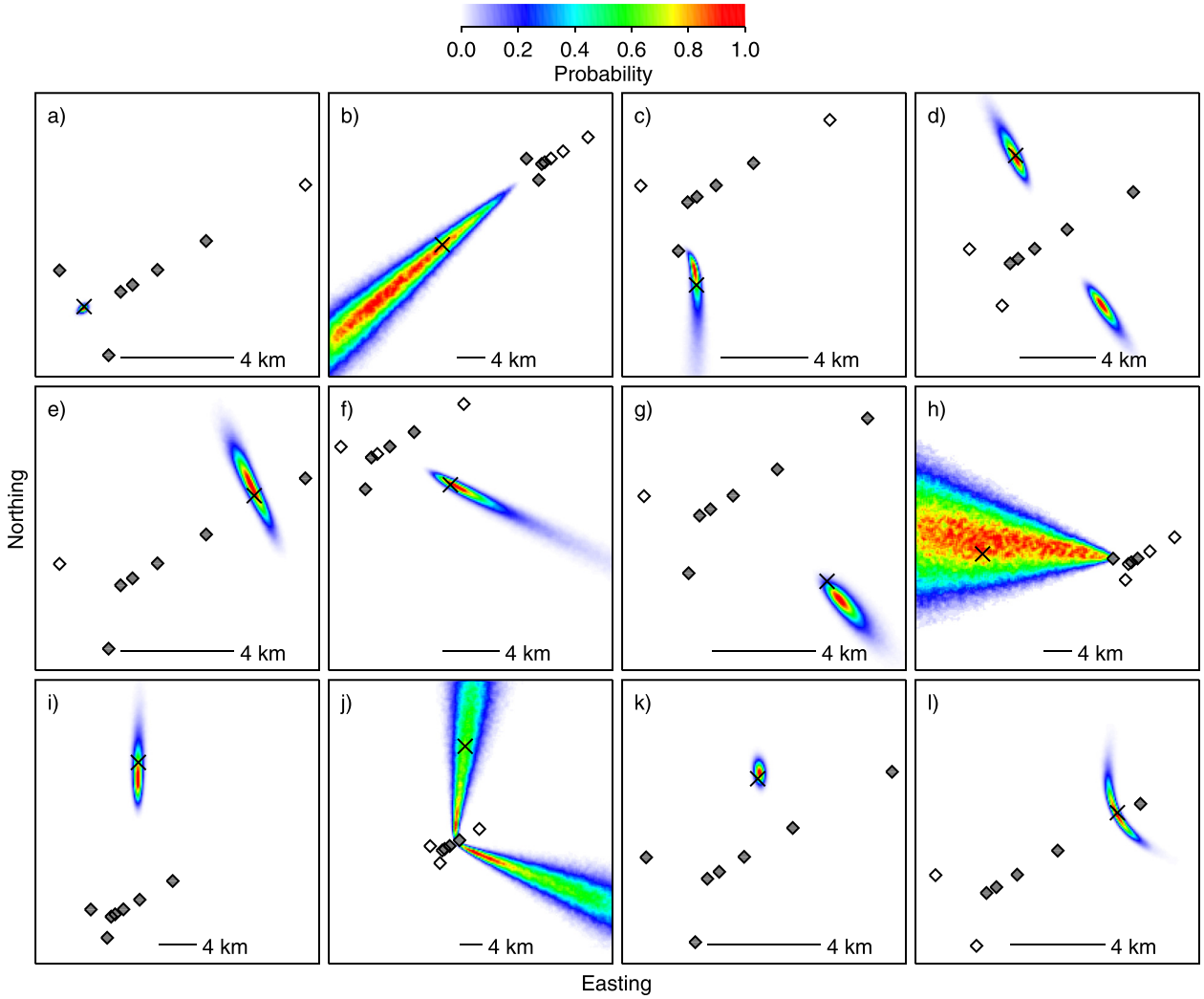

FIG. 7. (Color online) Amplitude-normalized marginal probability densities of bowhead whale locations for 12 selected calls. *A priori* AMAR locations (GPS deployment positions) are shown with diamond symbols; filled diamonds indicate AMARs with corresponding annotations, open diamonds represent AMARs without associated call annotations. MAP whale locations are shown with "×" symbols.

predicted TDOA data in excellent agreement with the synthetic data. The data fit to calls in simulations 1 and 3 and to other calls in simulation 2 were similar and are not shown for brevity.

V. CHUKCHI SEA WHALE LOCALIZATION RESULTS

The Bayesian inversion was applied to six batches of bowhead whale-call TDOA data from different half-hour periods of the recordings (referred to as scenarios S1–S6, Table II). We do not expect the relative recorder clock offsets to change significantly over these half-hour periods. The reported accuracy for the AMAR clocks is 10 ppm, which is equivalent to ∼18 ms over 30 min. Hence, we expect relative clock drifts between two receivers over 30 min to be 0–36 ms (this expectation is confirmed by the ambient-noise analysis presented later in this section). These relative drifts are generally small compared to the TDOA data (e.g., for a whale in line with the closest recorder pair the TDOA is about 486 m/1400 m/s = 350 ms). The simulations showed that localization results are not significantly affected by assuming a single call-independent effective waveguide sound speed so we use that parameterization in the bowhead whale call inversions. The inversions were carried out on a desktop computer using a single 4.4 GHz central processing unit. Convergence was reached after collecting approximately 200 000 PPD samples, which took between 1 and 10 h depending on the scenario (generally, scenarios with more calls and TDOA data took longer). The inversions were found to produce approximately Gaussian-distributed data residuals that were independent of time (not shown).

Figure 6 shows the MAP whale locations and one-standard deviation (1SD) uncertainty estimates for each scenario. We show uncertainty estimates for only ten (randomly selected) calls in each panel for clarity. The uncertainty estimates are aligned along the principle axes of the posterior covariance matrix and extend one standard deviation from the MAP locations. In some cases the error bars are not discernible because they are smaller than the plotted symbols indicating the MAP localization estimate; for these calls, the symbols are filled with black. Figure 6 shows that whales that are close to the array are generally well localized in two

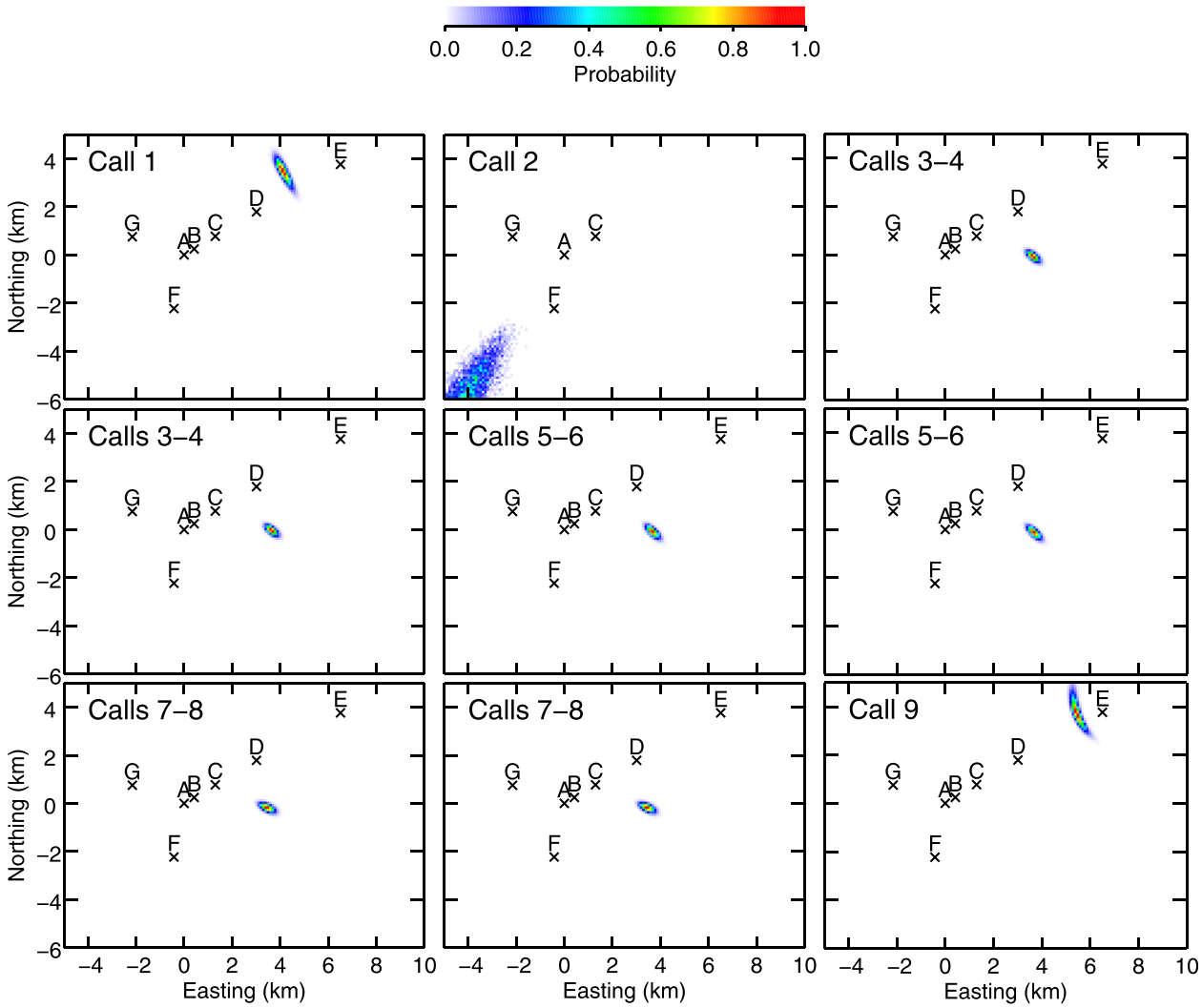

FIG. 8. (Color online) Amplitude-normalized marginal probability densities of bowhead whale locations from S6 for the same calls as analyzed using modal dispersion data in Warner *et al.* (Ref. 26). Call numbers on each panel correspond to call numbers in Warner *et al.* (Ref. 26). Note that the marginal density for call 2 extends away from the AMARs to the boundary formed by the minimum easting and northing prior (−30 km).

dimensions while distant whales typically have good bearing (or cross-range) estimates but poor range estimates. These uncertainty estimates provide an idea of the quality of the localizations but do not fully characterize the uncertainties due to the nonlinearity of the problem. Many of the 2D marginal probability densities for whale locations overlap, making them difficult to display on the same plot. For brevity, we only show a few (12) examples of localization marginals to illustrate the variety of PDF shapes in Fig. 7. Location uncertainty tends to increase with distance from the center of the AMAR cluster. When the off-axis recorders do not record a call, the probability densities are symmetric about the cluster axis [Figs. 7(d), 7(j), and 7(l)]. These three PPDs illustrate the potentially strong non-linearity of the inverse problem, i.e., location PDFs are non-Gaussian and can be multi-modal [e.g., Fig. 7(d)]. Resolving multi-modal PPDs required parallel tempering to provide sufficient sampling of all modes. The direction (bearing) of arrival for calls at long ranges is generally well determined but the range to the cluster is poorly constrained [Figs. 7(b) and 7(h), and to a lesser degree, Figs. 7(f) and 7(i)]. The non-Gaussian PPDs make it difficult to provide meaningful uncertainty estimates in terms of range or easting/northing standard deviation for all calls. However, half of the calls (173) had MAP locations within 6 km of the centroid of the array and the location PPDs were often well-constrained in easting and northing and appeared approximately Gaussian [e.g., Figs. 7(a) and 7(k)]. The median easting and northing standard deviations of these relatively close-range calls were about 170 m.

Although the true whale locations are not known for comparison, the TDOA localization results here can be compared to the modal-dispersion localization results from Warner *et al.*[26] for nine calls in S6, which were included in both studies. The marginal PDFs for whale locations from these calls are shown in Figs. 8 and 9 for the TDOA and modal-dispersion data, respectively. Marginal probability

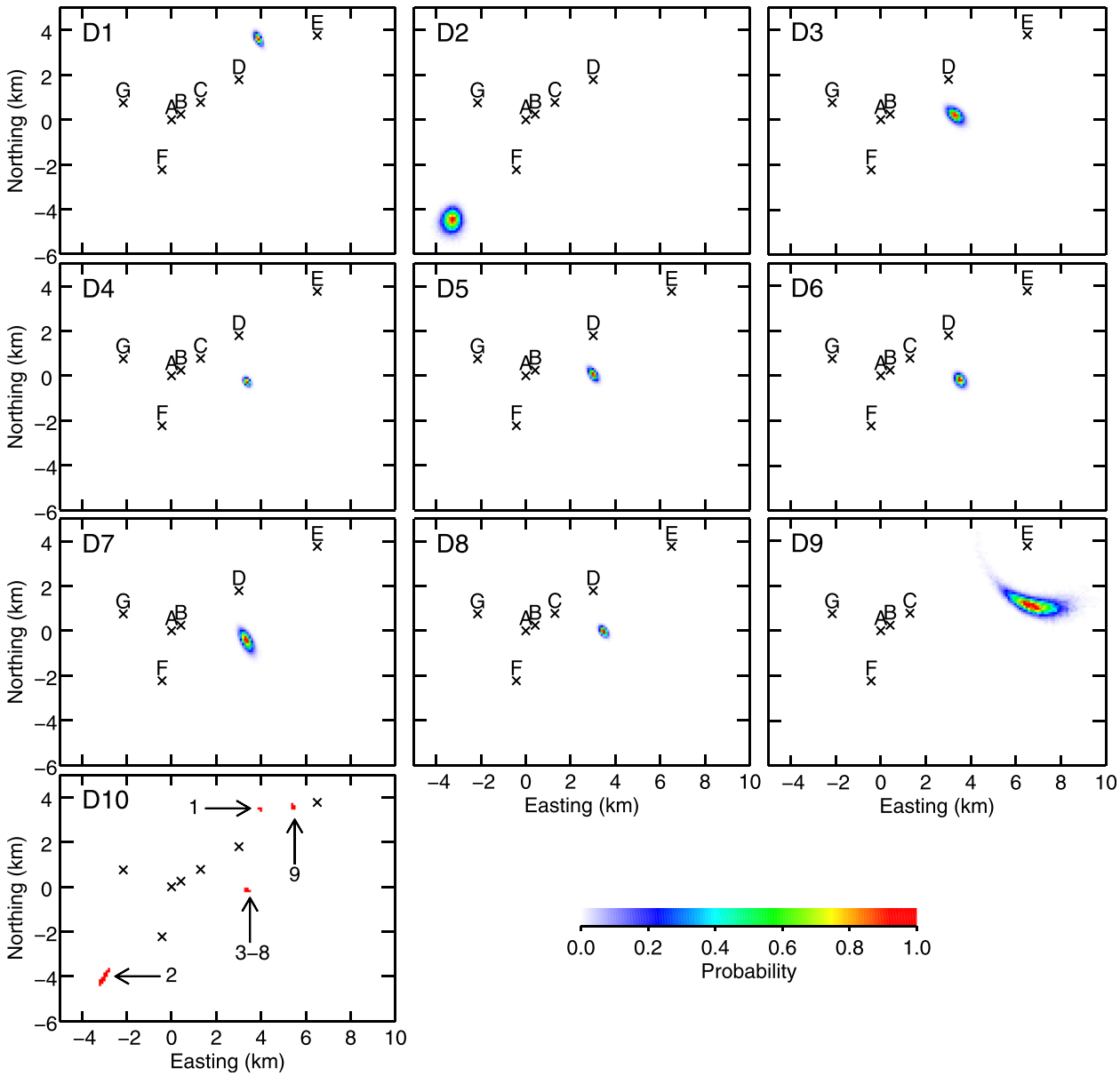

FIG. 9. (Color online) Amplitude-normalized marginal probability densities of bowhead whale locations from Ref. 26. Dispersion data from calls 1–9 were inverted individually (D1–D9) and jointly (D10). TDOA data from the same calls were inverted for the whale locations, as shown in Fig. 8.

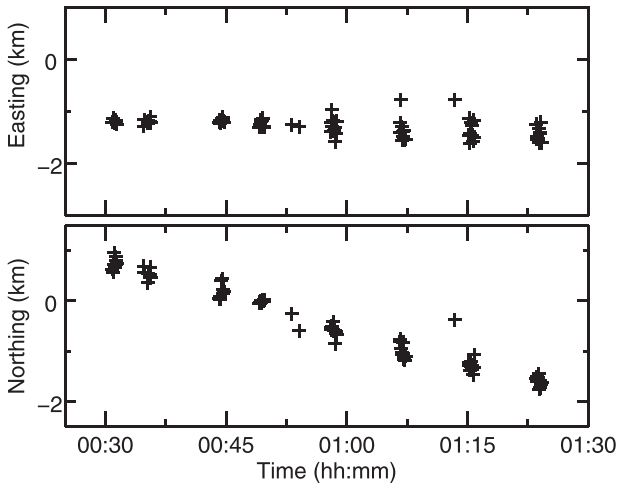

FIG. 10. Whale easting and northing vs time (on 27 September 2013) from the MAP models in S1–S3. The clusters of whale locations are likely from a whale (or whale group) traveling at ∼3 km/h.

densities for pairs of calls (3–4, 5–6, and 7–8) are duplicated in Fig. 8 because the annotations for the TDOA analysis encompassed both calls, treating the call pairs as single calls. Marginal densities for dispersion inversion of calls 1–9 are shown in Fig. 9 on panels D1–D9, and a joint dispersion inversion of all nine calls is shown in panel D10. In general, the TDOA-based locations agree well with the modal-dispersion based estimates, and have uncertainties that are comparable or slightly larger, providing confidence in the TDOA inversion scheme developed in this paper. One example where the TDOA data provide significantly less location information is for call 2; the range to the array is uncertain here via TDOA inversion but is well resolved by the modal-dispersion data. Also note that the TDOA-based location for call 9 corresponds best with the dispersion-based location from the joint (multi-call) inversion. The TDOA inversion performed better for this call than the individual-call dispersion inversion because the relative recorder clock offsets were better resolved in the TDOA inversion (but still not as well resolved as in the joint dispersion inversion).

The numerous whale location estimates close to AMARs A, F, and G in S1–S3 shown in Fig. 6 form a roughly north–south oriented line. The call times can be estimated by rearranging Eq. (1) for τ_w using the call annotation time for t_{wi}, resulting in slightly different estimates from each AMAR. For the following analysis, we set the times for each call to the mean of the call times estimated from each AMAR. Figure 10 shows the whale easting and northing vs time for S1–S3. The median easting and northing standard deviations for the calls in Fig. 10 are 103 and 116 m, respectively. The locations estimated from periodic bursts of calls appear to indicate a whale (or whale group) traveling southward at ∼3 km/h, a reasonable (although somewhat slow) speed for migrating bowhead whales.[47]

To consider the non-localization parameters estimated in the TDOA inversion, Table III lists the mean sound speed, relative recorder clock offsets, and residual error standard deviations with uncertainties for S1–S6, as well as clock-offset estimates from a modal-dispersion inversion[26] for a shorter time window within that of S6. Figure 11 shows the corresponding marginal probability densities for S6 (corresponding figures for S1–S5 are similar and omitted for brevity). The average effective waveguide sound speed is 1403 ± 18 m/s (1SD). The sound speed corresponds approximately with the average mode group speeds expected for the measurement environment for the frequencies of the annotated bowhead whale calls (approximately 1430 and 1380 m/s for modes 1 and 2, respectively). The clock drifts are approximately linear over the scale of days (also see Fig. 12). The estimated clock offsets in S6 are similar to but not consistent (within two-standard deviation uncertainties) with those in Warner *et al.*[26] using whale-call dispersion inversion. The latter estimates are likely more accurate because the normal-mode model of dispersive propagation is more accurate and dispersion data are more informative than the straight-path time-of-flight model and TDOA data used in this paper (but also far more computationally expensive).

Figure 12 shows the mean clock offset estimates from the whale call inversion vs time compared with point estimates obtained from cross correlations of ambient noise.[20] For the latter, long-time (1–4 days) ambient noise cross-correlation functions (NCF) were estimated by averaging NCFs calculated from sequential 5-min recordings. Such long time-averages were required to build the NCF due to the relatively large recorder separations; however, over these long durations, the clocks drifted relative to each other. To account for this, relative clock drift rates were estimated from the clock offset inversion results (these varied from ∼11–54 ms/h) and the cross correlations were calculated after delaying each 5-min noise segment of the non-reference recorder using drift rates of ±10 ms/h from the inversion estimates with 1 ms/h increments. The acoustic

TABLE III. Estimated effective waveguide sound speed, relative AMAR clock offsets, and residual error standard deviations, all with corresponding 1SD uncertainties for the bowhead whale call inversions. Clock offset estimates from a previous study (Ref. 26) during a smaller time window of S6 are also included.

Scenario	c (m/s)	Δ_B (s)	Δ_C (s)	Δ_D (s)	Δ_E (s)	Δ_F (s)	Δ_G (s)	σ (s)
1	1454,9	20.42,0.027	79.70,0.037	44.17,0.049	42.45,0.081	42.20,0.044	37.93,0.079	0.10,0.005
2	1421,24	20.42,0.026	79.66,0.029	44.01,0.049	42.19,0.174	42.35,0.046	37.96,0.049	0.10,0.004
3	1322,21	20.42,0.028	79.54,0.034	43.87,0.058	42.32,0.215	42.70,0.045	38.19,0.041	0.13,0.017
4	1422,12	21.93,0.029	87.30,0.026	48.05,0.034	47.35,0.050	46.94,0.029	41.33,0.031	0.13,0.003
5	1429,22	22.73,0.034	91.24,0.038	50.18,0.056	50.08,0.089	49.33,0.050	43.10,0.038	0.14,0.006
6	1370,15	24.09,0.022	97.97,0.023	53.79,0.049	54.76,0.101	53.37,0.031	46.01,0.024	0.13,0.005
Reference 26	–	24.04,0.002	97.84,0.002	53.54,0.005	54.39,0.013	53.16,0.004	45.87,0.003	–

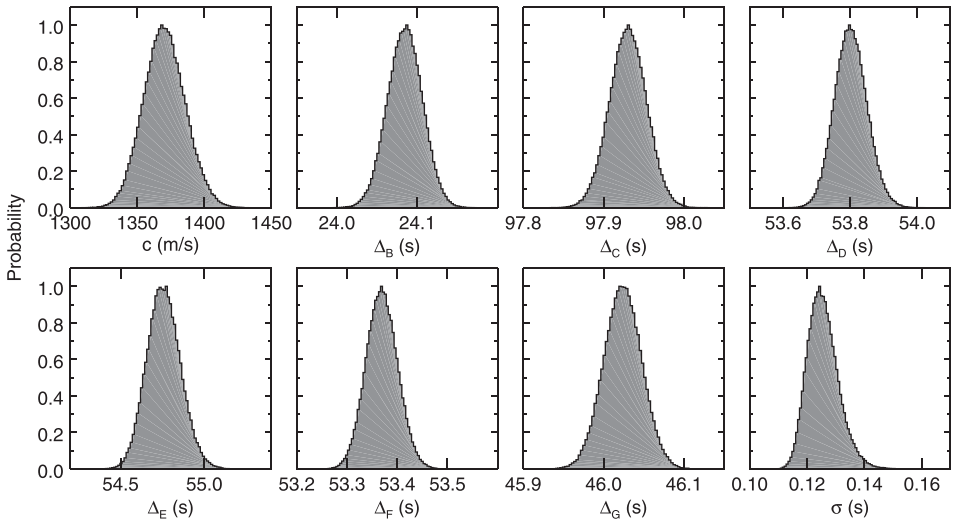

FIG. 11. Amplitude-normalized marginal probability densities for effective sound speed, relative recorder clock offsets, and residual error standard deviation estimated from the bowhead-whale call TDOA data in S6.

noise segments were bandpass filtered between 50 and 250 Hz and clipped to reduce the influence of transient noise events (e.g., bowhead whale calls). Only some NCFs (time period and drift rate combinations) showed the expected double-peak structure (at ± the acoustic travel time between receivers) and were suitable for estimating clock drift, likely because vessel noise violated the uniform noise source distribution assumption for some time segments. For each time period that resulted in the double-peak structure, only the NCF with strongest double peaks over all trial drift rates was saved for analysis. Clock offset estimates were obtained from the average of the lags corresponding to the two peaks of the derivative of the NCF. Figure 13 shows an example of the derivative of the NCF obtained from a one-day averaged NCF on 6 October 2013, with AMARs A and B, assuming a relative clock drift rate of 11 ms/h for AMAR B. Although the function is not perfectly symmetric about the average of the peak lags, the relative recorder clock offset can still be estimated to sufficient accuracy for comparison with the whale-call inversion results. The clock offsets from all suitable NCF derivatives are shown in Fig. 12 with circles and agree well with the TDOA estimates.

The effective waveguide sound speed can also be estimated by dividing the GPS-based AMAR separation distance by the two-way travel-time (TWTT). Table IV lists the NCF-based speeds and their uncertainties with the speeds estimated on the same days from the TDOA inversions (Table III). The NCF speed uncertainties were estimated assuming recorder easting and northing standard deviation of 25 m (i.e., based on the prior bounds in Table I representing two standard deviations), which corresponds to 35 m uncertainty in the receiver separation distance. This distance was converted to a percentage of the AMAR separation distance, which also applied to the sound speed (assuming no uncertainty in the TWTT, which likely leads to underestimating the sound speed uncertainties). The NCF- and TDOA-based speeds are consistent within two-standard deviation uncertainties.

Finally, the fit to the TDOA data achieved by the Bayesian inversion is illustrated in Fig. 14 for the first four calls in S1 with the observed TDOAs and the 5th and 95th percentiles for estimated TDOAs, calculated from a random sample of 5000 models from the PPD. The data index on the *x*-axis represents TDOA data from different AMAR pairs.

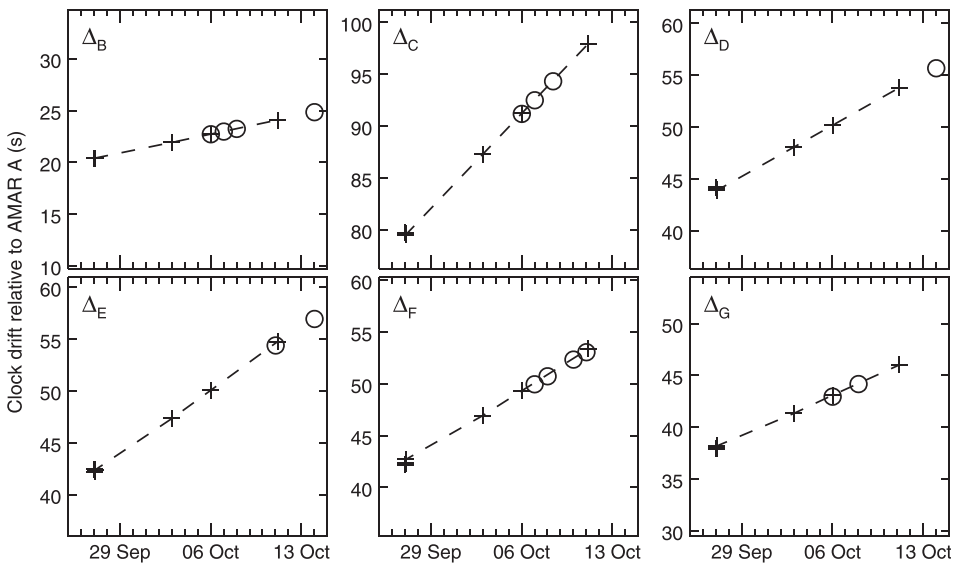

FIG. 12. Relative recorder clock offset vs time estimated from the TDOA inversion (+) and using ambient noise (○).

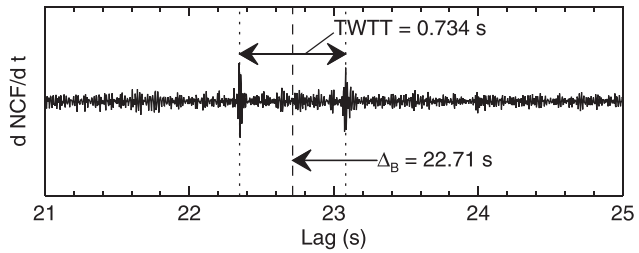

FIG. 13. Time derivative of the one-day time-averaged NCF between AMARs A and B from 6 October 2013. Dotted lines indicate peak times of the envelope of the derivative of the NCF and the dashed line indicates the relative recorder clock offset (i.e., average of the two peak times).

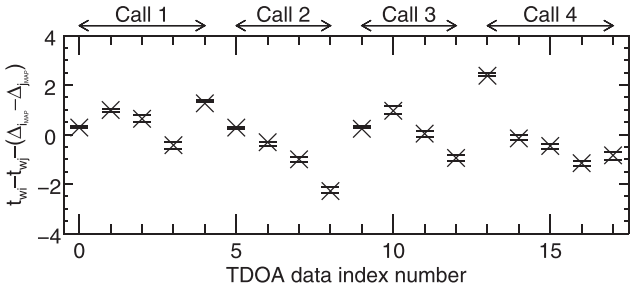

FIG. 14. Measured (×) and predicted (–) TDOA data (s) for bowhead-whale calls 1–4 in S1, reduced by the difference in relative recorder clock offsets from the MAP model. Predicted data are shown for the 5th and 95th percentiles of TDOA data from a random sample of the PPD.

The observed and estimated TDOAs were reduced by the difference of the MAP clock-offset estimates so the percentile differences are perceptible. The inversion sampled models that produced predicted TDOAs that are in good agreement with the measured data. The data fit to other calls and scenarios were qualitatively similar and are not shown for brevity; however, Table III lists the residual error standard deviation statistics for all scenarios. The estimated error standard deviations varied from about $\sigma = 0.10-0.14$ s.

VI. SUMMARY AND CONCLUSION

This paper developed and presented Bayesian inversion of bowhead-whale call TDOA data from recordings on an asynchronous hydrophone cluster in the Chukchi Sea. Calls were first manually detected, annotated, and associated between recorders, and then TDOAs were calculated by cross-correlating filtered waveforms. Linearly dependent data with lower peak cross-correlation values were not included in the inversion. This data filtering was necessary for obtaining rigorous uncertainty estimates in the Bayesian inversion (which assumed independent errors) and also reduced the influence on TDOA data of modal dispersion, which was not accounted for in the straight-path, time-of-flight propagation model. The TDOA data were used to estimate the whale locations, effective waveguide sound speed, relative recorder clock offsets, receiver locations, data error statistics, and uncertainties of all parameters.

A simulation study based on the recorder geometry of the Chukchi Sea acoustic measurement program illustrated the effects on localization results of a call-independent effective waveguide sound speed assumption and the degree to which model parameters could be estimated. Inversions of simulated data sets generated for call-dependent and call-independent sound speeds showed relatively little difference in terms of localization results, indicating that a call-independent assumption is appropriate for this problem (the treatment of sound speed may be more critical for inversions of time-of-arrival data with synchronized recorders than for TDOA data). Whale locations and clock offsets were reasonably well determined, but the sound speed and receiver locations were poorly resolved within their prior bounds. However, including sound speed and receiver locations as unknowns accounted for their uncertainties in the localization uncertainties. The source-receiver geometry had a large effect on whale location uncertainties and the PPD showed nonlinear effects including multi-modal structure and left-right ambiguities for whale locations in some cases.

TABLE IV. Estimated effective waveguide sound speeds from ambient noise cross correlation derivatives and the TDOA inversions on the same dates. Uncertainties are specified as plus or minus one standard deviation.

Date (scenario)	Recorder pair	Recorder separation distance (m)	NCF speed (m/s)	TDOA speed (m/s)
6 Oct (5)	AB	486 ± 35	1323 ± 96	1429 ± 22
6 Oct (5)	AC	1510 ± 35	1347 ± 32	1429 ± 22
6 Oct (5)	AG	2282 ± 35	1414 ± 22	1429 ± 22
11 Oct (6)	AE	7519 ± 35	1387 ± 7	1370 ± 15
11 Oct (6)	AF	2272 ± 35	1441 ± 22	1370 ± 15

The inversion of bowhead whale-call TDOA data from recordings in the Chukchi Sea showed similar effects to the simulation study. Whale-location uncertainties were generally smaller for calls originating closer to the center of the receiver cluster. Some calls were well localized in two dimensions whereas other calls were well resolved in bearing (or cross-range) but poorly resolved in range to the cluster. Bowhead-whale locations estimated from TDOA data agreed well with previous estimates using modal-dispersion data,[26] although the location uncertainties were typically larger for the TDOA data and the TDOA-based inversion does not provide estimates of the whale call source instantaneous frequency, water column sound speed profile, or seabed geoacoustic profiles. A sequence of calls received over a one-hour period were localized and appear to represent the track of a whale (or whale group) traveling at ∼3 km/h. Relative recorder clock offsets were estimated at several times spanning a two-week period and showed approximately linear drift rates. Estimated clock offsets and effective waveguide sound speeds agreed with estimates obtained by long-time cross correlations of ambient noise.

Overall, the inversion approach applied in this paper estimated marine-mammal locations with easting and northing standard deviation uncertainties of ∼170 m from calls made within 6 km of a large-aperture array of unsynchronized recorders. The method requires diversity of whale locations and minimal clock drift during the analysis time window. The approach can be used to estimate marine mammal spatial density or to track individuals (or groups). The

inversion is suitable to automatically detected and associated marine-mammal calls, allowing analysis of large data sets.

ACKNOWLEDGMENTS

The authors thank Michael Macrander and Koen Broker of Shell Exploration and Production Company and Shell Global Solutions, respectively, for allowing us to publish results from the Chukchi Sea study. G.A.W. was supported by JASCO Applied Sciences and a Natural Sciences and Engineering Research Council (NSERC), Canada, Industrial Postgraduate Scholarship.

[1]C. R. Greene, M. W. McLennan, R. G. Norman, T. L. McDonald, R. S. Jakubczak, and W. J. Richardson, "Directional frequency and recording (DIFAR) sensors in seafloor recorders to locate calling bowhead whales during their fall migration," J. Acoust. Soc. Am. **116**, 799–813 (2004).
[2]A. M. Thode, K. H. Kim, S. B. Blackwell, C. R. Greene, C. S. Nations, T. L. McDonald, and A. M. Macrander, "Automated detection and localization of bowhead whale sounds in the presence of seismic airgun surveys," J. Acoust. Soc. Am. **131**, 3726–3747 (2012).
[3]S. H. Abadi, A. M. Thode, S. B. Blackwell, and D. R. Dowling, "Ranging bowhead whale calls in a shallow-water dispersive waveguide," J. Acoust. Soc. Am. **136**, 130–144 (2014).
[4]Y.-T. Lin, A. E. Newhall, and J. F. Lynch, "Low-frequency broadband sound source localization using an adaptive normal mode back-propagation approach in a shallow-water ocean," J. Acoust. Soc. Am. **131**, 1798–1813 (2012).
[5]A. E. Newhall, Y.-T. Lin, J. F. Lynch, M. F. Baumgartner, and G. G. Gawarkiewicz, "Long distance passive localization of vocalizing sei whales using an acoustic normal mode approach," J. Acoust. Soc. Am. **131**, 1814–1825 (2012).
[6]R. A. Walker, "Some intense, low-frequency, underwater sounds of wide geographic distribution, apparently of biological origin," J. Acoust. Soc. Am. **35**, 1816–1824 (1963).
[7]W. A. Watkins and W. E. Schevill, "Sound source location by arrival-times on a non-rigid three-dimensional hydrophone array," Deep-Sea Res. Oceanogr. Abstr. **19**, 691–706 (1972).
[8]W. A. Watkins and W. E. Schevill, "Listening to Hawaiian spinner porpoises, *Stenella cf. Longirostris*, with a three-dimensional hydrophone array," J. Mammal **55**, 319–328 (1974).
[9]W. C. Cummings and D. V. Holliday, "Passive acoustic location of bowhead whales in a population census off Point Barrow, Alaska," J. Acoust. Soc. Am. **78**, 1163–1169 (1985).
[10]A. S. Frankel, C. W. Clark, L. M. Herman, and C. M. Gabriele, "Spatial distribution, habitat utilization, and social interactions of humpback whales, *Megaptera novaeangliae*, off Hawai'i, determined using acoustic and visual techniques," Can. J. Zool. **73**, 1134–1146 (1995).
[11]K. M. Stafford, C. G. Fox, and D. S. Clark, "Long-range acoustic detection and localization of blue whale calls in the northeast Pacific Ocean," J. Acoust. Soc. Am. **104**, 3616–3625 (1998).
[12]V. M. Janik, S. M. Van Parijs, and P. M. Thompson, "A two-dimensional acoustic localization system for marine mammals," Marine Mam. Sci. **16**, 437–447 (2000).
[13]C. W. Clark and W. T. Ellison, "Calibration and comparison of the acoustic location methods used during the spring migration of the bowhead whale, *Balaena mysticetus*, off Pt. Barrow, Alaska, 1984–1993," J. Acoust. Soc. Am. **107**, 3509–3517 (2000).
[14]R. P. Morrissey, J. Ward, N. DiMarzio, S. Jarvis, and D. J. Moretti, "Passive acoustic detection and localization of sperm whales (*Physeter macrocephalus*) in the tongue of the ocean," Appl. Acoust. **67**, 1091–1105 (2006).
[15]E. M. Nosal and L. N. Frazer, "Track of a sperm whale from delays between direct and surface-reflected clicks," Appl. Acoust. **67**, 1187–1201 (2006).
[16]P. B. Muanke and C. Niezrecki, "Manatee position estimation by passive acoustic localization," J. Acoust. Soc. Am. **121**, 2049–2059 (2007).
[17]X. Li, Z. D. Deng, L. T. Rauchenstein, and T. J. Carlson, "Contributed review: Source-localization algorithms and applications using time of arrival and time difference of arrival measurements," Rev. Sci. Instrum. **87**, 041502 (2016).
[18]J. L. Spiesberger, "Probability distributions for locations of calling animals, receivers, sound speeds, winds, and data from travel time differences," J. Acoust. Soc. Am. **118**, 1790–1800 (2005).
[19]A. Širović, J. A. Hildebrand, and S. M. Wiggins, "Blue and fin whale call source levels and propagation range in the Southern Ocean," J. Acoust. Soc. Am. **122**, 1208–1215 (2007).
[20]K. G. Sabra, P. Roux, A. M. Thode, G. L. D'Spain, W. S. Hodgkiss, and W. A. Kuperman, "Using ocean ambient noise for array self-localization and self-synchronization," IEEE J. Ocean. Eng. **30**, 338–347 (2005).
[21]A. M. Thode, P. Gerstoft, W. C. Burgess, K. G. Sabra, M. Guerra, M. D. Stokes, M. Noad, and D. H. Cato, "A portable matched-field processing system using passive acoustic time synchronization," IEEE J. Ocean. Eng. **31**, 696–710 (2006).
[22]B. Møhl, M. Whalberg, and A. Heerfordt, "A large-aperature array of non-linked receivers for acoustic positioning of biological sound sources," J. Acoust. Soc. Am. **109**, 434–437 (2001).
[23]Y. Simard and N. Roy, "Detection and localization of blue and fin whales from large-aperature autonomous hydrophone arrays: A case study from the St. Lawrence Estuary," Can. Acoust. **36**, 104–110 (2008).
[24]B. Miller and S. Dawson, "A large-aperature low-cost hydrophone array for tracking whales from small boats," J. Acoust. Soc. Am. **126**, 2248–2256 (2009).
[25]B. Miller, S. Dawson, and R. Vennell, "Underwater behavior of sperm whales off Kaikoura, New Zealand, as revealed by a three-dimensional hydrophone array," J. Acoust. Soc. Am. **134**, 2690–2700 (2013).
[26]G. A. Warner, S. E. Dosso, D. E. Hannay, and J. Dettmer, "Bowhead whale localization using asynchronous hydrophones in the Chukchi Sea," J. Acoust. Soc. Am. **140**, 20–34 (2016).
[27]J. Bonnel, A. M. Thode, S. B. Blackwell, K. Kim, and A. M. Macrander, "Range estimation of bowhead whale (*Balaena mysticetus*) calls in the arctic using a single hydrophone," J. Acoust. Soc. Am. **136**, 145–155 (2014).
[28]P. J. Green, "Reversible jump Markov chain Monte Carlo computation and Bayesian model determination," Biometrika **82**, 711–732 (1995).
[29]S. M. Wiggins, M. A. McDonald, L. M. Munger, S. E. Moore, and J. A. Hildebrand, "Waveguide propagation allows range estimates for North Pacific right whales in the Bering Sea," Can. Acoust. **32**, 146–154 (2004).
[30]L. M. Munger, S. M. Wiggins, and J. A. Hildebrand, "North Pacific right whale up-call source levels and propagation distance on the southeastern Bearing Sea shelf," J. Acoust. Soc. Am. **129**, 4047–4054 (2011).
[31]S. H. Abadi, W. S. D. Wilcock, M. Tolstoy, T. J. Crone, and S. M. Carbotte, "Sound source localization technique using a seismic streamer and its extension for whale localization during seismic surveys," J. Acoust. Soc. Am. **138**, 3951–3963 (2015).
[32]J. Delarue, J. MacDonnell, B. Martin, X. Mouy, and D. Hannay, "Northeastern Chukchi Sea joint acoustic monitoring program 2012-2013," Technical Report 00808, JASCO Applied Sciences (2014), available at https://www.chukchiscience.com/Portals/0/Public/Science/AcousticMoorings/2013_CSESP_Acoustics_Final_Report.pdf (Last viewed January 29, 2017).
[33]N. Metropolis, A. Rosenbluth, M. Rosenbluth, and A. T. A. E. Teller, "Equations of state calculations by fast computing machines," J. Chem. Phys. **21**, 1087–1092 (1953).
[34]W. K. Hastings, "Monte Carlo sampling methods using Markov chains and their applications," Biometrika **57**, 97–109 (1970).
[35]C. J. Geyer, "Markov chain Monte Carlo maximum likelihood," in *Computing Science and Statistics: Proceedings of the 23rd Symposium on the Interface*, Interface Foundation, Fairfax Station, VA (1991), pp. 156–163.
[36]A. Jasra, D. A. Stephens, and C. Holmes, "Population-based reversible jump Markov chain Monte Carlo," Biometrika **94**, 787–807 (2007).
[37]J. Dettmer and S. E. Dosso, "Trans-dimensional matched-field geoacoustic inversion with hierarchical error models and interacting Markov chains," J. Acoust. Soc. Am. **132**, 2239–2250 (2012).
[38]S. E. Dosso, C. W. Holland, and M. Sambridge, "Parallel tempering for strongly nonlinear geoacoustic inversion," J. Acoust. Soc. Am. **132**, 3030–3040 (2012).
[39]S. Dosso and M. Wilmut, "Uncertainty estimation in simultaneous Bayesian tracking and environmental inversion," J. Acoust. Soc. Am. **124**, 82–97 (2008).
[40]W. R. Gilks, S. Richardson, and D. J. Spiegelhalter, eds., "Markov Chain Monte Carlo in Practice," in *Interdisciplinary Statistics* (Chapman and Hall/CRC, London, 1996), pp. 1–486.
[41]M. Sambridge and K. Mosegaard, "Monte Carlo methods in geophysical inverse problems," Rev. Geophys. **40**, 3-1–3-29, doi:10.1029/2000RG000089 (2002).

[42]W. J. Teague, M. J. Carron, and P. J. Hogan, "A comparison between the Generalized Digital Environmental Model and Levitus climatologies," J. Geophys. Res. **95**, 7167–7183, doi:10.1029/JC095iC05p07167 (1990).
[43]M. R. Carnes, "Description and evaluation of GDEM-V 3.0," Technical Report 733009-9165, Naval Research Laboratory, Stennis Space Center, MS Oceanography Division (2009).
[44]T. J. Weingartner, "Vessel collected, C. T. D., NE Chukchi Sea 2008-2013 (Ed5)" (2013), available at https://workspace.aoos.org/group/6316/project/6626/folder/6634/, Alaska Ocean Observing System, Ocean Workspace (Last viewed February 11, 2015).
[45]C. F. Mecklenbräuker and P. Gerstoft, "Objective functions for ocean acoustic inversion derived by likelihood methods," J. Comput. Acoust. **8**, 259–270 (2000).
[46]E. K. Westwood, C. T. Tindle, and N. R. Chapman, "A normal mode model for acousto-elastic ocean environments," J. Acoust. Soc. Am. **100**, 3631–3645 (1996).
[47]S. E. Moore and R. R. Reeves, "Distribution and movement," in *The Bowhead Whale*, edited by J. J. Burns, J. J. Montague, and C. J. Cowles (Society for Marine Mammalogy, 1993), Vol. 2, pp. 313–388.